International Journal of Architectural, Civil and Construction Sciences
ISSN: 2415-1734
Vol:11, No:11, 2017

Analysis and Design of Offshore Triceratops under Ultra-Deep Waters

Srinivasan Chandrasekaran, R. Nagavinothini

***Abstract*—**Offshore platforms for ultra-deep waters are form-dominant by design; hybrid systems with large flexibility in horizontal plane and high rigidity in vertical plane are preferred due to functional complexities. Offshore triceratops is relatively a new-generation offshore platform, whose deck is partially isolated from the supporting buoyant legs by ball joints. They allow transfer of partial displacements of buoyant legs to the deck but restrain transfer of rotational response. Buoyant legs are in turn taut-moored to the sea bed using pre-tension tethers. Present study will discuss detailed dynamic analysis and preliminary design of the chosen geometric, which is necessary as a proof of validation for such design applications. A detailed numeric analysis of triceratops at 2400 m water depth under random waves is presented. Preliminary design confirms member-level design requirements under various modes of failure. Tether configuration, proposed in the study confirms no pull-out of tethers as stress variation is comparatively lesser than the yield value. Presented study shall aid offshore engineers and contractors to understand suitability of triceratops, in terms of design and dynamic response behaviour.

***Keywords*—**Buoyant legs, dynamic analysis, offshore structures, preliminary design, random waves, triceratops.

I. Introduction

DEEP sea oil exploration and production is increasing in the recent past. Several new generation platforms came into existence due to the quest for innovative and efficient structures. Offshore triceratops is one such new generation platform which shows adaptability to ultra-deep water conditions [3]. Triceratops can be installed at ultra-deep water depths ranging from 1500 m to 3000 m [2]. The construction and installation of triceratops are cost effective and hence the platform is suggested for ultra-deep water conditions [20]. These structures practically extend the fixed platform performance to ultra-deep water. It derives an advantage through the chosen geometrical form [4]. The conceptual model of triceratops is shown in Fig. 1. Triceratops consists of deck, which is connected to three buoyant legs by a ball joint arrangement. The buoyant legs are then position restrained by a set of taut moored tethers. The innovative component in the triceratops that adds advantage for efficient operation in ultra-deep water conditions under extreme sea state is the ball joint. The ball joint restrains the transfer of rotational motion from buoyant legs to deck and allows only the translation motion to be transferred. This behaviour reduces the response of deck in adverse environmental conditions and impose comfortable working environment to people on board. The other important structural component of triceratops is buoyant legs. These are deep draft structures similar to that of spar platform and are designed as stiffened-cylindrical shell structures [10]. The efficient orthotropic system was used in the design of buoyant legs, as the primary load path to resist the external pressure [1]. Buoyant legs possess reliable performance characteristics; they are simple to fabricate, transport and install in deep waters [11]. Studied conducted on buoyant leg structures had shown its evolution to produce a platform carrying a large deck load [15].

Srinivasan Chandrasekaran, Professor, is with the Department of Ocean Engineering, IIT Madras, Chennai 600036, India (corresponding author; e-mail: drsekran@iitm.ac.in).

R.Nagavinothini, PhD Research Scholar, is with the Department of Ocean Engineering, IIT Madras, Chennai 600036, India (e-mail: vino.civil35@gmail.com).

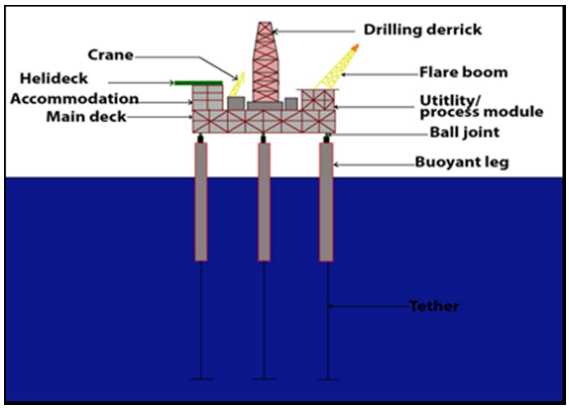

Fig. 1 Conceptual Model of triceratops

Recent research on triceratops under deep water conditions had shown the advantages of structural configuration and good re-centering capability of platform and also suggested that triceratops can be seen as an effective alternative for ultra-deep waters [6]. Studies also revealed that the coupled response of the deck in rotational degrees-of-freedom is lesser than that of buoyant legs [7]. The pitch response of deck is lesser than that of buoyant legs under seismic excitation conditions also [5]. Under strongly asymmetric waves, the response of triceratops was lower in magnitude showing beat phenomenon in all degrees of freedom [8]. The modified form of triceratops with stiffened buoyant legs had shown significant increase in the tether tension [9]. The orientation of the platform also becomes important as it influences the tether tension variation [2]. Improved dry tree access is possible in triceratops through better motion characteristics, which is one of the salient advantages [5]. Previous researchers had studied the response of the triceratops up to a water depth of 1000 m [8], [16], [17]. As offshore industry is moving towards ultra-

deep waters in the recent years, it becomes mandatory to report the adequacy of the new generation platform like triceratops in ultra-deep water conditions.

Assessment of nonlinear response of compliant platforms under random waves is important to determine the maximum stresses and deformations [18]. Though many analytical and experimental studies were carried out in the recent past on triceratops, they shall not be considered as the validation of proof for the design applications. In addition, it is well known that the minor changes in the design considerations will affect the response of the offshore platforms in deep waters adversely. The current study is focused on the preliminary design of buoyant legs and deck for the triceratops at a water depth of 2400 m. Numerical analysis is carried out under irregular waves. The response of the platform under different sea states and wave approach angle are also presented. As tethers are one of the crucial components in taut moored systems like triceratops, stress analysis of tethers is also carried out under different sea states and wave approach angles. This study is the preliminary investigation to check the effectiveness of triceratops for ultra-deep water and the risers were not considered in the dynamic analysis. The main aim of the study is to prove the efficiency of this new generation platform in ultra-deep water condition with due importance to design considerations of crucial components.

II. Preliminary Design of Triceratops

Since triceratops is in the development stage, the model for ultra-deep waters is developed on the basis of dimensions of PERDIDO spar [13]. The height and topside weight of the platform is maintained same as that of the spar platform. The height of buoyant legs is 174.24 m and the diameter is 15 m. The topside weight is 97400 kN. The buoyancy is distributed to three buoyant legs, based on which the diameter of buoyant legs is derived. The details of triceratops are given in Table I. As the platform has three buoyant legs, equilateral triangular shaped deck of side length 95 m is chosen for enhancing symmetry. The superstructure is designed with three deck levels.

A. Buoyant Legs

The buoyant legs are designed as orthogonally stiffened cylindrical shells to resist the axial load and bending moment with lateral pressure. The preliminary design of buoyant legs is carried out for the intermediate environmental conditions (7.9 m wave height and 9.1 seconds peak period) found in Gulf of Mexico [1]. The cylindrical shell with ring frames and stiffeners are designed with high strength steel. The orthogonally stiffened cylinders are also called as ring-stringer stiffened cylinders. The ring frames and longitudinal stiffeners are attached internally to the cylinder at particular distant apart. The cylindrical shell is provided with 70 stringers and ring frames at 3m apart, designed as flat bars of 300 x 40 mm. The stiffeners are integrally welded to the cylindrical shell and it resists the lateral loading. Heavy ring frames are also provided at the end of the cylindrical shell. The design is controlled by the stresses developed in the operating condition and the stiffened cylindrical shell is checked for shell buckling, panel stiffener buckling, panel ring buckling, general buckling and column buckling as per DNV-RP-C202 [19]. Though this method is considered empirical, there is a good agreement between the experimental and theoretical values. However, finite element analysis is required at the detailed design stage for the potential output. In the preliminary design, the effect of geometric imperfections and residual stresses are not considered. The conceptual model of the buoyant leg with stiffeners is shown in Fig. 2.

TABLE I
Details of Triceratops

Description	Unit	Quantity
Water Depth	m	2400
Unit Weight of Material	kg/m^3	7850
Unit weight of Sea water	kg/m^3	1025
Geometric Details		
Diameter of Leg	m	15
c/c distance between the legs	m	61.77
Length of the Leg	m	174.24
Freeboard	m	20.24
Draft	m	154
Tether length	m	2246
Diameter of tether	m	1.00
Vertical Centre of gravity of buoyant leg	m	-112.74
Metacentric Height	m	35.83
Load Details		
Self-weight + payload	kN	562424
Buoyancy force	kN	820932
Total Tether force	kN	258491
Structural properties		
Area of deck	m^2	3933
Area of tether	m^2	2.356
Stiffness of tethers	GN/m	0.22

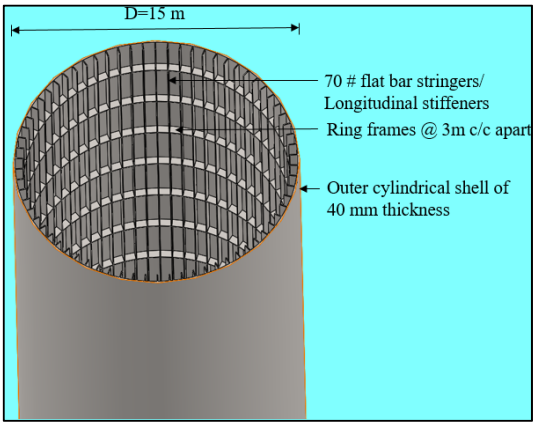

Fig. 2 Conceptual model of buoyant leg

B. Deck

The topside is designed with three deck levels such as cellar deck, main deck and top deck. The integrated truss deck system is designed with the floor made up of truss type connection for the main deck flooring and other decks are provided with beam panel arrangement. The load from the top

deck is transferred to main deck through longitudinal and transverse tubular members and stiffened with diagonal members to resist the wind loads [14]. Every component is designed based on the bending moment developed on the respective component. The deck floor details are given in Table II.

TABLE II
DESIGN CONSIDERATIONS OF DECK

Description	Value
Shape of the deck	Triangular deck
Length of the deck	95 m
Number of decks	3
Number of bays in the truss	9
Length of each bay	9.5 m
Load Details	
Total Topside weight	97.4 MN
Live load in process and drilling zone	5 kN/m^2
Live load in storage floors	18 kN/m^2
Sustained wind speed	55.88 m/s
Initial tether tension	28721.143 kN
Design Considerations	
Factor of safety for deal and live load	1.3
Type of steel	High strength steel
Size of deck components	
Thickness of deck plate	100 mm
Transverse beam	Wide flange beam W 27 x114
Longitudinal beam	Back to back channel section stiffened with flange plates: Web = 700 x 30 mm Flange = 350 x 30 mm
Open web joist type	k-series
Depth of web joist	710 mm
Diameter of web joist members	20 mm
Main chord members of truss	Channels, back to back
Diagonal members of truss	Tubular members
Diameter and thickness of diagonal members	800 mm; 12 mm
D/t ratio of truss diagonal members	40

III. NUMERICAL MODELLING AND FREE OSCILLATION STUDIES

The numerical model is developed using ANSYS AQWA solver, in order to overcome the difficulties arising due to modelling and simulation of offshore platform with six degrees of freedom. This solver simulates the Linearized hydrodynamic fluid wave loading by three dimensional radiation theory or diffraction theory. In time domain dynamic simulation, the aqwa analysis simulates the real time motion of a floating body at each time step by integrating the accelerations in time domain by predictor-corrector numerical integration scheme. The buoyant legs are modelled as Morison elements and the wavelength of the sea states are maintained as greater than five times the diameter of the buoyant legs. They are defined as TUBE elements in aqwa and the fluid force acting on the member is calculated by the Morison's equation [17].

$$q_n = \frac{1}{2}\rho C_d dA(v_n - \dot{x}_n)|v_n - \dot{x}_n| + \rho dV a_n + (C_m - 1)\rho\, dV(a_n - \ddot{x}_n) \quad (1)$$

where, C_d is drag coefficient, C_m is the inertia coefficient, ρ is the density of sea water, dA and dV are the exposed area and displaced volume per unit length respectively; v_n and a_n are water particle velocity and acceleration respectively; $\dot{x}_n$ and $\ddot{x}_n$ are velocity and acceleration of the structure. The inertia and drag coefficients are taken as 1.0 and 0.75 respectively, which could be approximated for a normal sized cylindrical tube. The hydrodynamic forces are then calculated by three point Gaussian integration scheme. The origin lies in the still water level and the wave forces are estimated by accounting the influence of variable submergence effect. The buoyant legs are connected to the deck by ball joints and the buoyant legs are position restrained by taut moored tethers, which are modelled as linear cables ignoring. Followed by the development of model, meshing of deck is carried out with quadrilateral and triangular panels by three dimensional panel method. The hydrostatic analysis is performed on the numerical model and it shows that the meta-centric height lies above the centre of gravity. The initial pretension in the tethers is assigned in aqwa through the stiffness and the unextended length of the tether. The numerical model is shown in Fig. 3. The following equation of motion is solved by convolution integration technique:

$$[M + M_a]\ddot{x}(t) + [C]\dot{x}(t) + [K]x(t) = F(t) \quad (2)$$

where, $\ddot{x}(t)$, $\dot{x}(t)$, $x(t)$ and F(t) are acceleration, velocity, displacement and force vectors, [M] is the structural mass matrix, M_a is the added mass matrix, [C] is the damping matrix and [K] is the stiffness matrix.

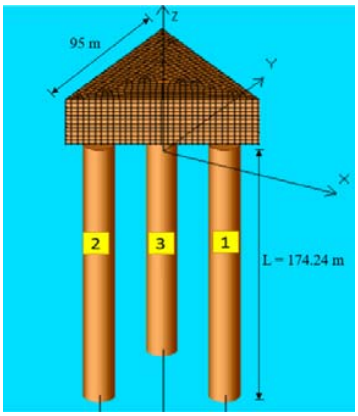

Fig. 3 Numerical Model of Triceratops

Free Oscillation studies are carried out for the tethered triceratops to find the natural period of the platform in six degrees of freedom, by giving external disturbing forces. Then the damping ratio is calculated by logarithmic decrement method. Table III shows the natural period and damping ratio of triceratops in six degrees of freedom. The obtained results are compared with the experimental results of stiffened

triceratops [7]. It shows that the triceratops have high degree of compliancy in surge and sway degrees of freedom. The natural periods of the platform modelled in the present study is higher than that of the values in literature, in all degrees of freedom. In the present study, lesser damping ratio is obtained in the translational degrees of freedom and higher values are obtained in rotational degrees of freedom, as compared to the literature. The discrepancies in the natural period and damping ratio may be attributed to the difference in the type of buoyant legs and water depth considered in the studies. The reduction in the damping ratio leads to the increase in the natural period in translational degrees of freedom and vice versa in rotational degrees of freedom.

TABLE III
NATURAL PERIOD AND DAMPING RATIO OF TETHERED TRICERATOPS

Degree of Freedom	Present Study		Reference study [7]	
	Natural period (s)	Damping ratio (%)	Natural period (s)	Damping ratio (%)
Surge	215.0	5.84	88.4	8.15
Sway	215.4	5.87	88.4	8.15
Heave	4.3	0.94	1.8	1.08
Roll	6.2	6.11	9.46	4.34
Pitch	6.1	6.10	9.46	4.34
Yaw	215.9	6.23	-	-

IV. DYNAMIC RESPONSE ANALYSIS UNDER RANDOM WAVES

TABLE IV
CHARACTERISTICS OF SEA STATES

Sea state description	Significant wave height (m)	Zero crossing period (s)
Moderate sea state	6.5	8.15
High sea state	10	10
Very High sea state	15	15

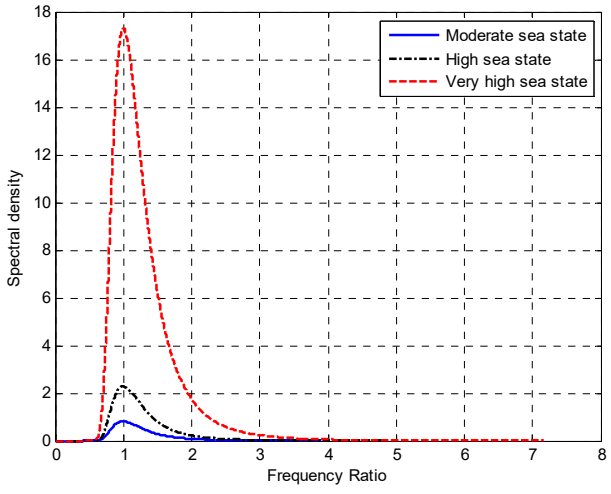

Fig. 4 PM spectrum for different sea states

Waves play a critical role in the design of offshore compliant structures due to the complications involved in the hydrodynamic behaviour of the platform in open sea conditions. Ocean waves are a combination of waves of different frequencies and directions. In order to model the ocean waves, simplified theories and spectra models are available in the literature. The random waves are represented by wave spectra, which spread from zero to infinite frequencies. However, wave energy is found to be concentrated on a narrow band. The exciting forces due to wave loading are evaluated by a nonlinear drag force term. The different sea states considered for the dynamic analysis are given in Table IV.

Pierson Moscowitz (PM) spectrum is used for representing the wave energy distribution under different frequencies. The typical wave energy spectruö under different sea states is shown in Fig. 4. It is two parameter spectrum suitable for open sea conditions, which is neither fetch limited nor duration limited. It is developed under moderate winds over large fetches [16]. PM spectrum is formulated by significant wave height and average wave period.

$$S^{+}(\omega) = \frac{1}{2\pi}\frac{H_s{}^2}{4\pi T_z{}^2}\left(\frac{2\pi}{\omega}\right)^2 \exp\left(-\frac{1}{\pi T_z{}^4}\left(\frac{2\pi}{\omega}\right)^4\right) \quad (3)$$

where, H_s is the significant wave height, T_z is the zero crossing period and ω is the frequency.

A. Response under Different Sea States

TABLE V
DECK RESPONSE UNDER DIFFERENT SEA STATES

Sea state	Statistics	Surge	Heave	Pitch
Moderate	Maximum	2.3006	0.0053	0.0297
	Minimum	-2.0943	-0.0147	-0.0160
	Mean	0.0301	-0.0015	0.0009
	Standard Deviation	0.6545	0.0023	0.0040
	RMS	0.6552	0.0028	0.0041
High	Maximum	6.478	0.0059	0.1145
	Minimum	-5.034	-0.1059	-0.0487
	Mean	0.123	-0.0083	0.0022
	Standard Deviation	1.654	0.0117	0.0101
	RMS	1.659	0.0144	0.0103
Very high	Maximum	22.571	0.0083	0.6116
	Minimum	-20.178	-1.8165	-0.2515
	Mean	0.929	-0.2406	0.0189
	Standard Deviation	6.736	0.2858	0.0815
	RMS	6.799	0.3736	0.0836

The response of the triceratops in different sea states under unidirectional waves are studied in surge, heave and pitch degrees of freedom. The response under other degrees-of-freedom is negligible. The wave is applied along the direction of x axis as shown in Fig. 3. The nature of the response is periodic in nature and it fluctuates around the mean position. The response statistics are given in Table V. The maximum response increases with the increase in the wave height in surge, heave and pitch degrees of freedom. In surge response, RMS value increases by 2.527 and 10.376 times in the high and very high sea state with respect to moderate sea state respectively. The increase in the roughness of sea also reflects in the response in all degrees of freedom, which can be predicted from the increase in standard deviation in different sea states. In heave response, the mean value decreases and

RMS value increases from moderate to very high sea states. Even in very high sea state, the maximum pitch response is found to be 0.6116 degrees. The RMS value in high and very high sea states increase by 2.512 and 20.9 times that of moderate sea state.

The power spectral density plot of deck surge and heave responses under different sea state are shown in Fig. 5. In moderate sea state, several peaks are observed in the surge and heave response of the deck. In surge response, the first peak occurs at the surge natural frequency and the maximum peak occurs at the peak wave frequency corresponding to the sea state. The second peak occurring at the frequency of 0.236 rad/s gets suppressed with the increase in the severity of the sea state. In heave response, the maximum peak occurs at the frequency very close to pitch natural frequency.

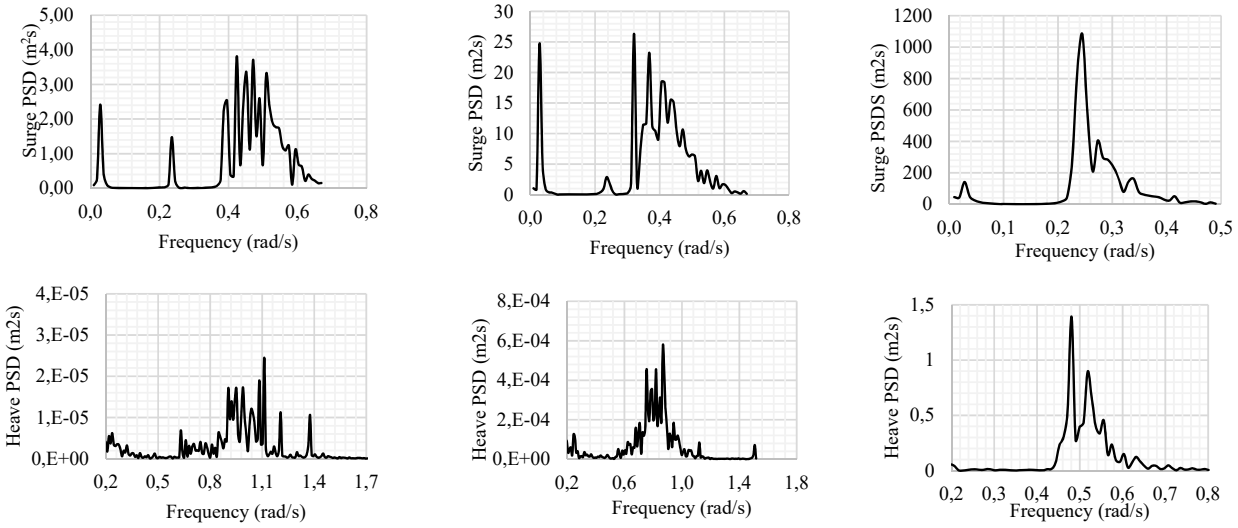

(a) Moderate sea state (b) High sea state (c) very high sea state

Fig. 5 Deck Surge and heave response in different sea states

Under high sea state, the first peak in surge response occurs at the surge natural frequency and the maximum peak corresponds to the peak wave frequency. In heave response, peak occurs at the frequency twice that of the peak wave frequency. In the surge response under very high sea state, the first peak occurs at the surge natural frequency and the second peak occurs at the frequency of 0.245 rad/s. In heave response, the peak occurs at a frequency of 0.4810 rad/s, one third of heave natural frequency. The heave response is lesser than that of surge response.

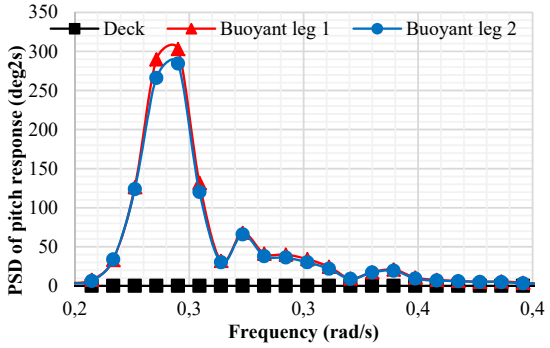

Fig. 6 Pitch response of deck and buoyant leg in very high sea state

The pitch response of deck and buoyant legs is shown in Fig. 6. The pitch response of deck is very low compared to that of the buoyant legs, which shows the efficiency of ball joint in restraining the rotational degrees of freedom. The maximum pitch response in the buoyant legs occurs at frequency of 0.245 rad/s. The pitch response of buoyant legs 2 and 3 remains same, due to symmetry. The maximum pitch response in deck is reduced by about 92.30% that that of buoyant leg in very high sea state. The complete restraint in the transfer of rotational degrees of freedom cannot be ensured, due to unequal heave response in three buoyant legs.

B. Validation of Results

The results obtained from the current numerical analysis are compared with the numerical study carried out on stiffened triceratops at a water depth of 215.78 m. The results obtained are validated in Table IV, for high sea state under unidirectional waves. It is observed that the heave response remains the same in both the cases and the pitch response of the triceratops in the current study is 48% lesser. This shows the advantage of triceratops in ultra-deep waters. In spite of increase in water depth, triceratops is showing excellent motion characteristics. Though there is an increase in the surge response in the present study, it is only about 1.08% of water depth. This may be attributed to the increase in the water depth and the difference in the type of buoyant leg

structure considered in the studies.

TABLE VI
VALIDATION OF RESULTS

Maximum deck response	Current study	Reference study [7]
Surge PSD (m^2s)	26.00	16.00
Heave PSD (m^2s)	0.00059	0.00058
Pitch PSD (deg^2s)	0.0000424	0.000088

C. Response under Different Wave Heading Angles

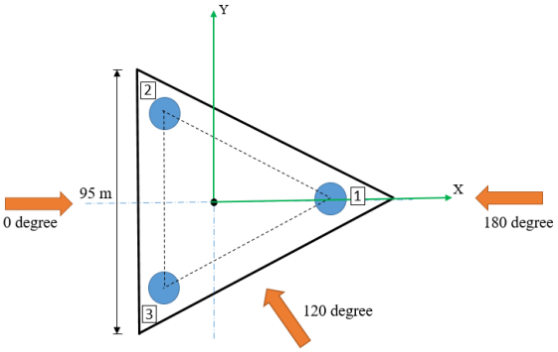

Fig. 7 Plan view of Triceratops with wave approach angles

In order to assess the realistic hydrodynamic interaction phenomena, incident wave load is applied at different angles i.e., 0 degree, 120 degree and 180 degree in very high sea state, as shown in Fig. 7. The deck response in different degrees of freedom is obtained. Significant response is seen in surge, sway and heave degrees of freedom as shown in Fig. 8. In surge response, first peak occurs at surge natural frequency and second peak occurs at frequency of 0.245 rad/s at all incident angles. The surge response remains same at 0 and 180° incident angles and at 120°, it reduces by 75%. Sway response is seen only at the incident angle of 120°. The peaks occur at the sway natural frequency and 0.245 rad/s. The heave response of deck remains same at all incident angles and the peak occurs at one third of heave natural frequency. The response remains very less in the rotational degrees of freedom, even at different incident wave angles due to the restraint offered by ball joints.

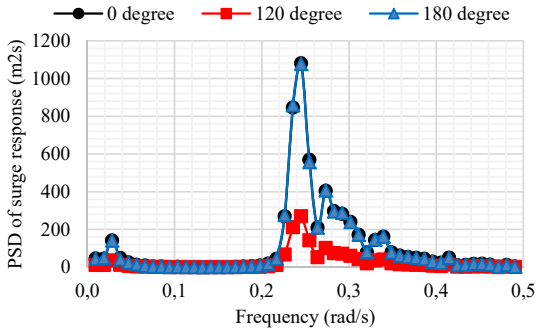

(a) Surge Response

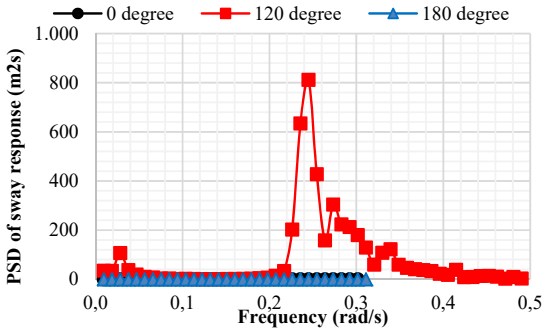

(b) Sway Response

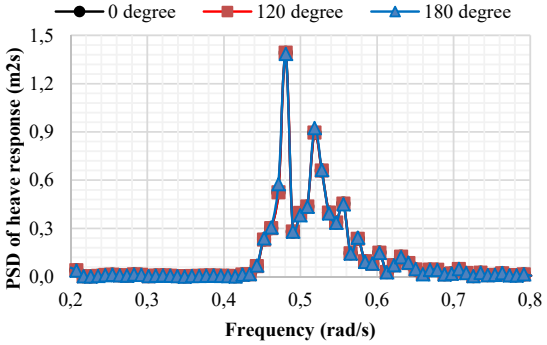

(c) Heave Response

Fig. 8 Deck surge, sway and heave response under different wave incident wave angles in very high sea state

The statistics of surge, sway and heave responses of deck under different incident angles are given in Table VII. The maximum surge response is seen at 0° incident angle. The sway response is close to zero at 0 and 180° incident angles and is prominently seen at the incident angle of 120°. The difference in the heave response under different incident angles is found out to be negligible.

TABLE VII
DECK RESPONSE (IN M) UNDER DIFFERENT WAVE INCIDENT ANGLES IN VERY HIGH SEA STATE

Incident angle	Statistics	Surge	Heave	Pitch
0 degree	Maximum	23.9114	-0.0039	0.0071
	Minimum	-15.8907	-0.0301	-2.2451
	Mean	1.2389	-0.0179	-0.3054
	Standard Deviation	7.3614	0.0057	0.3620
	RMS	7.4649	0.0187	0.4736
120 degree	Maximum	7.9228	20.7146	0.0067
	Minimum	-11.9742	-13.7623	-2.2436
	Mean	-0.6260	1.0574	-0.3054
	Standard Deviation	3.6802	6.3758	0.3620
	RMS	3.7331	6.4629	0.4736
180 degree	Maximum	15.5830	0.0053	0.0050
	Minimum	-23.6201	-0.0244	-2.3240
	Mean	-1.2389	-0.0141	-0.3064
	Standard Deviation	7.3680	0.0057	0.3639
	RMS	7.4714	0.0152	0.4758

Developing a model and simulation for a range of wave incident angles acting on the triceratops will predict the complete hydrodynamic interaction of platform. So, the numerical analysis is carried out with the range of wave incident angles from 0 to 120° degrees in very high sea state. The maximum deck response in the surge, sway and heave degrees of freedom are shown in Fig. 9. The response in the other degrees-of-freedom is found to be negligible. In surge degree of freedom, the maximum response decreases from 0 to 90° and then increases. In sway degree of freedom, the response behaviour is opposite to that of the surge response. The maximum surge and sway response are observed at 0 and 90°, respectively. In heave degree of freedom, the response remains same in the range of 30 to 90° and the maximum response is observed at 0°. The surge and sway response matches at the incident wave angle of 45° at which the heave response is also found to be lower.

V. Stress Analysis of Tethers

Each buoyant leg in the triceratops model is position restrained by a set of three tethers, 2246 m long with a core diameter of 100 mm. Tethers are usually manufactured as steel tubes or wired ropes of carbon steel or stainless steel. Stainless steel wires of small diameter are twisted around the central core to form a strand and number of strands is again twisted to form a tether. Each leg has 3 set of tethers.

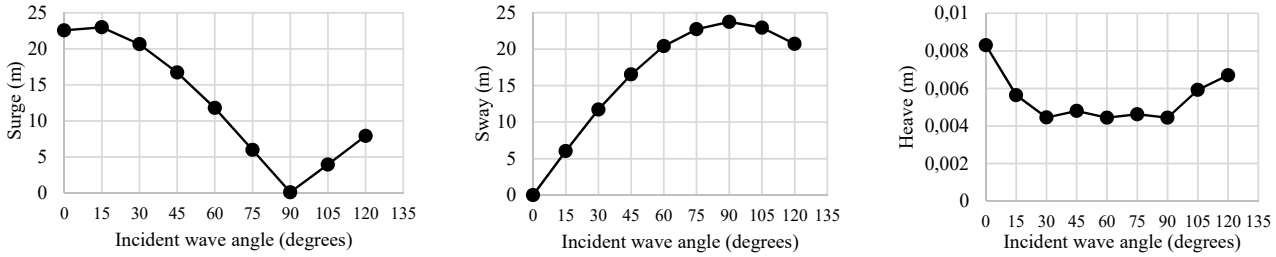

(a) Surge Response (b) Sway Response (c) Heave Response

Fig. 9 Maximum deck response in different wave approach angles in very high sea state

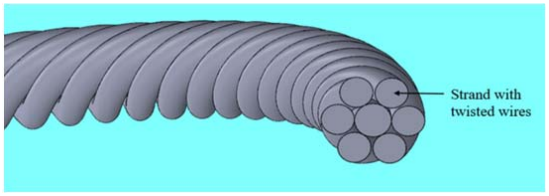

Fig. 10 Conceptual model of tethers

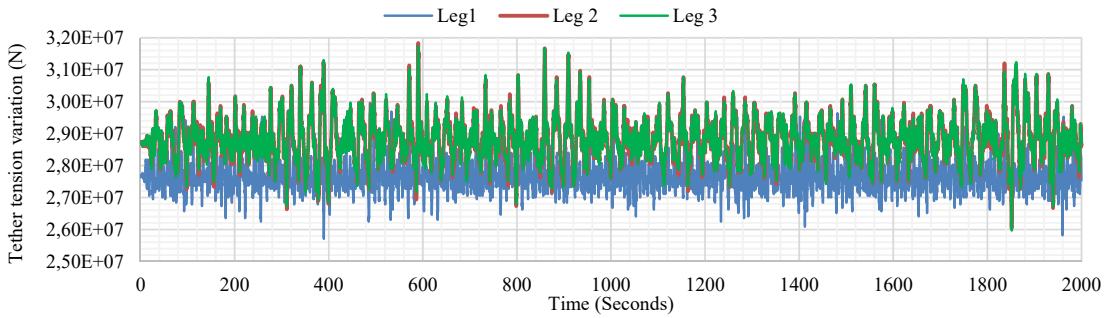

Fig. 11 Tether tension variation in very high sea state

The strength and ductility of each wire should be accounted for in the stress analysis study of tethers. Each tether in the model consists of high strength steel (7 x 52) with left lay regular lay arrangement. Each strand consists of 52 wires laid around the central core in opposite direction to the strands. The yield stress and breaking stress of wires are 500 MPa and 1500 MPa respectively. The initial pretension in each tether is 27.65 MN. The conceptual model of tethers is shown in Fig. 10.

A. Comparison Tether Tension in Different Sea States

Under the action of wave loads, each buoyant leg transfers the motion to the deck independently and this results in dynamic tether tension variation. The tether tension variation

is harmonic in nature. The difference in the tether tension variation among three buoyant legs is found out to be 2%. Hence, the tether tension variation statistics of buoyant leg 1 under different sea states is given in Table VIII.

Under moderate sea conditions, the maxima and minima are found out to be 29.47 MN and 26.30 MN respectively. The mean value shifts from the initial pretension by 0.02 MN and the tether tension variation is 5.73%. In high sea state, the tether tension variation increases to 7.68%. The change in the RMS value in different sea states is found to be negligible. In very high sea state, the mean value shifts form the initial pretension by 0.1 MN and the tether tension variation is 9.98%. The maximum stress developed in each wire of the tether under moderate, high and very high sea states are 12.02 MPa, 12.23 MPa and 12.40 MPa respectively. The stress developed in the wires is 2.48% of the yield stress. The tether tension variation and PSD plot under very high sea state of tethers in three buoyant legs are shown in Figs. 11 and 12 respectively. The maximum peaks occur at the peak wave frequency and the pitch natural frequency. A significant peak is also observed at 0.745 rad/s, which is 0.5 times of heave natural frequency. It is seen that the tether tension variation depends on the pitch and heave response of the buoyant legs under high sea state condition.

TABLE VIII
VALIDATION OF RESULTS

Statistics	Moderate	High	Very high
Maximum (MN)	29.474	29.958	30.388
Minimum (MN)	26.301	25.709	24.848
Mean (MN)	27.671	27.670	27.751
RMS (MN)	27.673	27.674	27.759
Tether tension variation (%)	5.73	7.68	9.98
Service Life of tethers in years	14.02	14.01	13.83

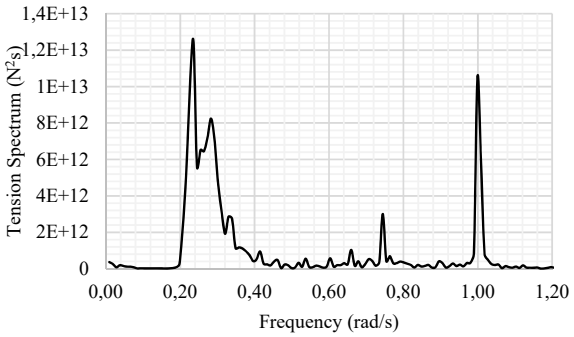

Fig. 12 Tether tension variation in very high sea state

Though the stress developed in the tethers are very low, tethers may undergo fatigue failure due to the periodic response of the tension variation. The fatigue analysis is also carried out by S-N curve approach, as per codal provisions [12]:

$$\log N = \log A - m \log S \quad (4)$$

where, N is the number of allowable cycles, S is the stress range, A and m are the constants obtained from the S-N curves. The fatigue parameters are chosen for the member in sea conditions and fatigue damage is calculated by Palmgren Miner's rule. Then, fatigue life estimated for 2000 seconds is extrapolated to find the service life of the tethers. The service life of the platform obtained under different sea states is given in Table VII. Though the variation in the service life of tethers is found out to be very small, it decreases with the increase in the severity of the sea state.

B. Comparison of Tether Tension in Different Wave Approach Angles

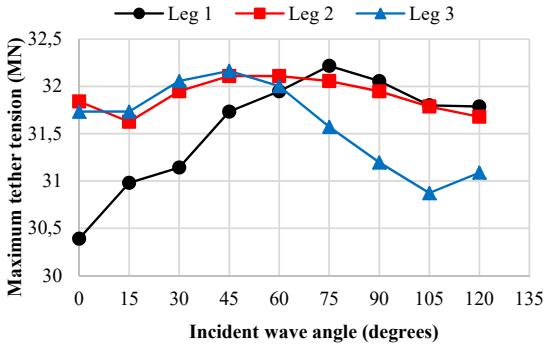

Fig. 13 Maximum tether tension of tethers in three buoyant legs

The difference in tether tension variation in three buoyant legs is mainly due to the wave incident angle. Fig. 13 shows the maximum tension developed in a tether in all three buoyant legs. In buoyant leg 1, the maximum tension increases till 75 degrees and then decreases. The maximum tension of tethers developed in buoyant leg 2 and buoyant leg 3 closely matches in the range of 0 degree to 60 degree; similarly, tension in buoyant leg 1 and buoyant leg 2 matches in the range of 60 degree to 120 degree. The tether tension in all three legs are found to be closer at the wave incident angle of 60 degrees and the maximum tension at this angle is found to be 15% greater than the initial pretension. Tether tension in buoyant leg 1 and buoyant leg 3 are comparatively less at the incident wave angles of 0 degrees and 120 degrees respectively. The variation in buoyant leg 2 is comparatively lesser than that of other two legs, in this range of wave incident angles.

VI. CONCLUSIONS

Current study examined the offshore triceratops under irregular waves in different sea states and incident angles. Unidirectional irregular wave represented by PM spectrum is considered. The preliminary design of buoyant legs confirms member level design requirements under various failure modes. Free floating analysis shows that there is a shift in the natural period of the structure from the wave period indicating the ease of installation under different sea states. The reduced heave response indicates the suitability of the platform for ultra-deep water conditions. The exclusive operational merit

of the platform is seen from the reduced pitch response of the deck, even under very high sea state. This is achieved due to the presence of ball joints. The lower stress variation in the tethers confirms no tether pull-out under harsh environmental conditions and the service life is also assessed through fatigue damage analysis. This detailed numerical analysis shows that triceratops can be said be an effective concept for ultra-deep waters. Since the waves are wind excited phenomenon, this study can be further extended to get the coupled response of triceratops under the action of wave and wind. In the detailed design stage, finite element analysis is required to predict the stresses developed in the deck and buoyant legs. This study serves as a prima facie in proving the efficiency of triceratops under ultra-deep water conditions.

REFERENCES

[1] Capanoglu, C.C., Shaver, C.B., Hirayama, H. and Sao, K., 2002, January. Comparison of model test results and analytical motion analyses for a buoyant leg structure. In The Twelfth International Offshore and Polar Engineering Conference. International Society of Offshore and Polar Engineers.

[2] Chandrasekaran, S., Sundaravadivelu, R., Pannerselvam, R., Madhuri, S. and Varthini, D.S., 2011, January. Experimental investigations of offshore triceratops under regular waves. In Proc. 30th International Conf. on Ocean, Offshore and Arctic Engg, OMAE.

[3] Chandrasekaran, S. and Seeram, M., 2012. Stability studies on offshore triceratops. International Journal of Innovative Research and Development, 1(10), pp.398-404.

[4] Chandrasekaran, S., Madhuri, S. and Jain, A.K., 2013. Aerodynamic response of offshore triceratops. Ships and Offshore Structures, 8(2), pp.123-140.

[5] Chandrasekaran, S. and Nannaware, M., 2014. Response analyses of offshore triceratops to seismic activities. Ships and Offshore Structures, 9(6), pp.633-642.

[6] Chandrasekaran, S., Mayank, S. and Jain, A., 2015, May. Dynamic response behavior of stiffened triceratops under regular waves: experimental investigations. In Paper presented at: Thirty Fourth International Conference on Ocean, Offshore and Arctic Engineering.

[7] Chandrasekaran S, Madhuri S. 2015. Dynamic response of offshore triceratops: Numerical and experimental investigations. Ocean Engineering. 109:401-409.

[8] Chandrasekaran S and Jamshed Nassery. 2015. Springing and ringing response of offshore triceratops. In: ASME 2015 34th International Conference on Ocean, Offshore and Arctic Engineering, St. Johns, Newfoundland, Canda; May31-June 5. p.1-6.

[9] Chandrasekaran S, Mayank S. 2017. Dynamic analyses of stiffened triceratops under regular waves: experimental investigations. Ships and Offshore Structures. 12(5):697-705.

[10] Chen Y, Zimmer RA, de Oliveira JG, Jan HY. 1985. Buckling and Ultimate Strength of Stiffened Cylinders: Model Experiments and Strength Formulations. In: Offshore Technology Conference, Houston, Texas; May 6-9. p. 113-124.

[11] Copple, R.W. and Capanoglu, C.C., 1995, January. A buoyant leg structure for the development of marginal fields in deep water. In The Fifth International Offshore and Polar Engineering Conference. International Society of Offshore and Polar Engineers.

[12] DNV DN. 2005. Fatigue design of offshore steel structures. Recommended practice DNV-RP-C203.

[13] Liapis, S., Bhat, S., Caracostis, C., Webb, C. and Lohr, C., 2010. Global performance of the Perdido spar in waves, wind and current–numerical predictions and comparison with experiments. OMAE2010-2116.

[14] Reddy, D.V. and Swamidas, A.S.J., 2013. Essentials of offshore structures: framed and gravity platforms. CRC press.

[15] Shaver, C.B., Capanoglu, C.C. and Serrahn, C.S., 2001, January. Buoyant leg structure preliminary design, constructed cost and model test results. In The Eleventh International Offshore and Polar Engineering Conference. International Society of Offshore and Polar Engineers.

[16] Srinivasan Chandrasekaran. 2015. Dynamic analysis and design of ocean structures. Springer, India, ISBN: 978-81-322-2276-7.

[17] Srinivasan Chandrasekaran. 2017. Dynamic analysis and design of ocean structures, Springer, 2nd Ed., Singapore.

[18] Tabeshpour, M.R., Golafshani, A.A. and Seif, M.S., 2006. Comprehensive study on the results of tension leg platform responses in random sea. Journal of Zhejiang University-Science A, 7(8), pp.1305-1317.

[19] Veritas, D.N., 2010. Buckling Strength of Shells, Recommended Practice DNV-RP-C202. Det. Nor. Ver. Class. AS, Veritasveien, 1.

[20] White CN, Copple RW, Capanoglu C. 2005. Triceratops: an effective platform for developing oil and gas fields in deep and ultra-deep water. In: The Fifteenth International Offshore and Polar Engineering Conference, Seoul, Korea; June 19-24. p. 133-139.